5G Antenna Characterization in the Far-Field

How close can Far-Field be ?

Benoît Derat
ROHDE & SCHWARZ GmbH & Co. KG
OTA and antenna test solutions R&D
Munich, Germany
benoit.derat@rohde-schwarz.com

***Abstract*—5G mobile devices and base stations will be operating antenna arrays and beam-steering techniques in the millimeter-wave region. The question of the far-field measurement distance is particularly critical for such technologies as a larger over-the-air test range means dynamic range issues and significantly larger cost. The traditionally used formula for the far-field distance aims at limiting the impinging field phase curvature. Using this criterion leads to testing distances of more than 6 meters to assess the far-field radiation pattern of a 5G smartphone equipped with 39 GHz transceiver. This paper investigates the physical relevance of such a large distance. It uses spherical wave expansion theory to establish two new far-field distance definitions, including considerations on the antenna directivity. An initial set of measurement data is provided to support the findings that much shorter distances than commonly known can be used for accurate far-field evaluation in the main radiation beam.**

Keywords—antenna; measurement; millimeter-wave; 5G; OTA.

I. Introduction

Far-field (FF) is generally considered to start at a distance r_{ff}=$2D^2/\lambda$, where λ is the wavelength and *D* is the maximum dimension of the radiation source. This criterion may however be overly conservative when the antenna occupies a very small volume of the radiating equipment. This case will exactly happen with mobile devices operating 5G New Radio (NR) at frequencies in the 28 and 39 GHz ranges [1]. Indeed, for future 5G handsets, chipset and mobile phone manufacturers are looking at arrays of patches or dipoles integrated into small modules, which are typically not more than a couple of cm large. For a 2cm-sized antenna array, r_{ff} gives a FF distance of ca. 8 cm at 28 GHz. For a 15cm-long mobile device, applying *D*=15 cm results in a FF distance of 4.2 m. Actual devices are however not completely covered with antenna arrays and the 2-cm antennas are made to essentially operate as standalone radiating elements. The FF behavior must hence start in space at a much shorter distance than 4.2 m. The question of "where?" then becomes crucial as the cost and complexity involved for over-the-air (OTA) measurement systems increases dramatically with the testing distance.

This contribution aims at providing a new angle of view on the FF distance matter. In particular, an analytical approach based on spherical wave expansion is used to demonstrate that the FF, identified by the separation of radial and angular variable dependences in the radiation pattern, occurs at a much closer range than r_{ff}. By taking into account the physical limit on directivity to quality factor ratio, a relation between the directivity and the start of the FF region is derived. Of course, with a shorter distance between the device under test (DUT) and the measurement probe, the uncertainty contribution due to the offset between the center of the measurement coordinate system and the apparent phase center increases. This impact is discussed hereafter. Measurements on a 5G NR antenna mock-up in a compact fully anechoic chamber are presented which corroborate the findings.

II. Far-Field Distance Background

When describing the behavior of the electromagnetic field created by an antenna, it is usual to distinguish between three concentric spherical regions encompassing the radiating source. In the reactive near-field region, the magnitude and phase variations of the field follow complex patterns which strongly depend on the fine structure of the antenna. So-called evanescent modes generate distribution changes which happen within small fractions of the wavelength. In the radiative near-field or Fresnel region, the evanescent modes have mostly vanished, yet the angular field distribution still depends on the distance from the antenna. Finally, the FF or the field in the Fraunhofer region has the following properties: its angular distribution is independent from the distance to the antenna, E and H field vectors are transverse to the direction of propagation and orthogonal to each other, and the impedance of the field |E|/|H| at each location approaches the free-space wave impedance of 120π Ohms.

Practical antenna performance assessments, at least in the field of wireless communications, are mostly about determining FF radiation characteristics. For enabling an accurate direct FF evaluation, the distance *R* from the measurement antenna to the DUT must first be sufficient to ensure that FF patterns from both the measurement antenna and the one under test are formed, in the sense that they have all the above-listed properties. In addition, taking aside environment reflections and interferences, the design of FF antenna test ranges is guided by criteria relating to the coupling between the DUT and measurement probe, the transverse and longitudinal amplitude tapers of the illuminating wavefront, as well as its phase curvature [2]. The reactive and reradiative couplings result only in minor errors when *R* is above 10λ. The most restrictive criteria are those on longitudinal amplitude taper and phase curvature. For the first one, supposing the antenna active region is of size *L*, and the center of this region

978-1-5090-5997-3/18/$31.00 ©2018 IEEE

occupies the center of the coordinate system of the test range, then the expected measurement error L_{err} can be written as [2]:

$$L_{err}[dB] = 20 \cdot log\left(\frac{R+L/2}{R-L/2}\right) \quad (1)$$

A distance R higher than $9L$ then ensures an error of less than 1 dB, while going down to 0.5 dB requires R greater than $18L$.

Finally, in a first-order approximation and at distances typically greater than D^2/λ, the field appears to propagate as a spherical wave emanating from the DUT phase center at the observation point. The phase deviations from the ideal far-field plane-wave spread across the measurement antenna aperture and create an error, mostly affecting the radiation pattern nulls, as well as the levels of the side lobes. The maximum phase difference $\Delta\varphi$ across an aperture of diameter D around the observation point has been calculated and presented in many books and papers, such as e.g. [2], [3]:

$$\Delta\varphi = \frac{\pi D^2}{4\lambda R} \quad (2)$$

A conventional choice is to bound $\Delta\varphi$ by $\pi/8$, which then results in the commonly adopted definition for the far-field distance $r_{ff} = 2D^2/\lambda$.

Three points are interesting to note about the phase curvature aspects. First, D is usually taken as the maximum DUT dimension, which is very conservative as the size which matters is that of the "active region" (the region with energetic radiating currents). As explained in I, this size may be much smaller than the DUT size in the case of 5G mobile devices. Second, the origin of measurement errors comes from phase variations across the measurement antenna aperture. This receiving aperture may also be much smaller than the DUT size and hence the phase variations be much smaller than (2) indicates. Nonetheless, as mobile devices are used in both transmit and receive mode, (2) is the relevant formula to apply. Third, despite r_{ff} is the commonly used FF distance, the limitation of phase curvature variations may be less restrictive than that imposed by longitudinal taper.

III. On the Formation of the Far-Field

Using spherical wave expansion theory, it has been demonstrated that modes of order n greater than $N=ka$, with k being the free-space wavenumber $2\pi/\lambda$ and $a=D/2$ the radius of the minimum sphere containing the antenna, have high quality factors at the surface of the considered sphere. As a result, these modes are typically unsolicited except in the case of "supergain" antennas [4]-[6]. Such antennas are narrowband and unpractical to implement in wireless mobile devices.

The dependence of the electric and magnetic fields on the radial distance r from the center of the coordinate system in which a spherical expansion is performed is determined by spherical Hankel functions (SHF) and their first derivatives, see e.g. [7]. The asymptotic forms of SHF are tabulated in [8]. For SHF of the second kind, the asymptotic form is given by:

$$h_n^{(2)}(kr) \sim \frac{1}{kr} e^{-j\left[kr - \frac{(n+1)}{2}\pi\right]} \quad (3)$$

The first derivative of the asymptotic function is also dominated by a $1/kr$ term, which is no surprise as both FF electric and magnetic fields are known to have a $1/kr$ dependence.
The asymptotic forms approach the actual functions in magnitude within less than ±5% for values of n such that $kr \geq n^2 + n$ [8]. In other words, at such a distance, the mode of order n has already reached its far-field behaviour. Taking then into account the spatial cut-off at $N=ka$, a new FF distance r_{ffm} can be defined which corresponds to an upper bound at which the field radiated by a non supergain antenna exhibits FF properties as listed in II:

$$r_{ffm} = \frac{2D^2}{\lambda}\left[\frac{\pi}{4} + \frac{1}{4}\frac{\lambda}{D}\right] \quad (4)$$

When $D \geq (4-\pi)\lambda$, r_{ffm} is smaller than r_{ff}. When D is large compared to λ, r_{ffm}/r_{ff} reaches its minimum of $\pi/4 \approx 79\%$.

IV. On the Relationship between Far-Field Distance and Directivity

Different calculations of an upper bound of the directivity U to quality factor Q ratio (U/Q) for arbitrary antennas have been introduced in [7], [9]. The maximum U/Q writes as follows:

$$\max(U/Q) = 2\sum_{n=1}^{\infty} \frac{2n+1}{Q_n + Q_n'} \quad (5)$$

Where Q_n and Q'_n are functions of ka defined as in [5] and relating to the quality factor of each spherical harmonic of order n. By having systematically evaluated the contribution of high order modes to the maximum achievable U/Q, it has been identified that modes of order higher than N_{dir} have a total influence on the upper bound of less than 0.5 dB, where N_{dir} equals:

$$N_{dir} = \lceil 1.0252 \cdot (ka)^{0.8633} \rceil \quad (6)$$

This formula yields exact results or conservative by only one additional mode compared to the results obtained from numerical implementation of (5) for ka up to 90. Fig. 1 illustrates this in the case of excited spherical modes of order 7 or less.

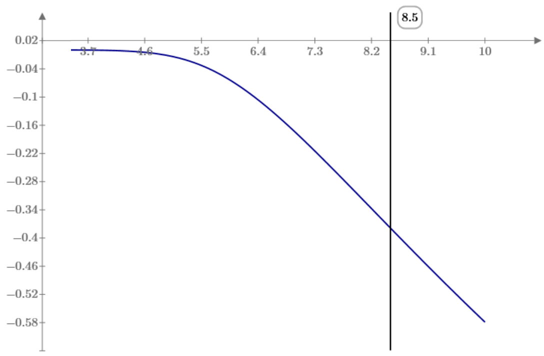

Fig. 1. Ratio (dB) of maximum achievable U/Q using spherical modes of order 7 or less to the maximum achievable U/Q using an infinity of modes, as a function of $x=ka$.

Fig. 2 shows the results of the systematic calculations for the 0.5 dB threshold of U/Q for ka up to 20, and justification for (6).

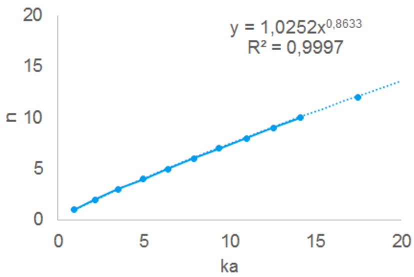

Fig. 2. Number of modes required to achieve the maximum U/Q bound minus 0.5 dB as a function of $x=ka$.

From a 5G NR handset antenna design perspective, the objective is to achieve the maximum possible directivity in a constrained antenna volume, while meeting fractional bandwidth requirements. In other words, the antenna design optimization for such an application naturally leads in the direction of using the lowest possible order modes to achieve the directivity goals. As higher order modes are also more “difficult” to excite energetically [5], [6], this is also the path of least development effort. It is hence unlikely that modes of order above N_{dir} are significantly solicited by real devices, so that the FF distance will then be imposed by the N_{dir} order modes. In such a case, a new realistic far-field distance is then established:

$$r_{ffD} = \lambda\left(\frac{\pi D}{\lambda}\right)^{0.8633}\left[0.1673\left(\frac{\pi D}{\lambda}\right)^{0.8633} + 0.1632\right] \quad (7)$$

Fig. 3 shows a comparison between r_{ff} and r_{ffD} at 24 and 43.5 GHz (resp. λ=1.25 and 0.69 cm), the mmW frequency bounds for 5G NR defined as FR2 (frequency range 2).

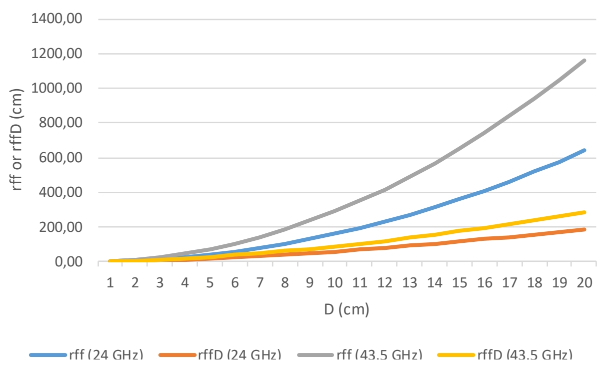

Fig. 3. Comparison between FF distance calculated according to formula (7) and classical r_{ff} as a function of D. x and y axis are in cm units.

r_{ffD} provides a much shorter distance than the classical r_{ff}. For example, a 5cm large antenna would be tested in the FF at 72.5 cm or more, according to r_{ff}. Taking into account the r_{ffD} definition of FF, a 27.2 cm distance would be sufficient. It is probably important to remind at this stage that r_{ff} and r_{ffD} do not subtend the same properties of the measured field. At distances $r \geq r_{ffD}$, the FF pattern is formed in the sense described in II. At distances $r \geq r_{ff}$, the phase variation within $\pm D/2$ around each point of observation over the sphere of radius r is smaller than π/8. The latter guarantees lower error in the magnitudes of the secondary lobes and the nulls of the pattern. The first one is enough to assess the main beam of the radiation pattern with less than 0.5 dB additional uncertainty. It is worth noting though that the longitudinal taper error increases when testing distance reduces. As an example, a 50 cm range length according to r_{ffD} enables a FF testing of the main beam of the DUT with an active region as large D=72 mm at 43.5 GHz. (1) then gives a 1.25 dB error, which would affect mostly secondary lobes if the center of the active region is at the center of the coordinate system.

V. Measurement Results

A. Measurement Setup

The fully anechoic chamber R&S®ATS1000 is used together with the Vector Network Analyzer (VNA) R&S®ZVA67 to perform measurements with a 28 GHz 5G NR antenna mock-up. The chamber is shown on Fig. 4. The inside absorbers tip-to-tip dimensions are 0.64m×1.25m×0.93m. The chamber contains a 0.03°-resolution conical cut system with a 360°-rotating azimuth table supporting the DUT and a 168°-rotating elevation arm moving the measurement probe. This setup allows covering the complete sphere except for a 12° cone around the pole towards the ground. The range length is tunable and is here adjusted so the measurement distance yields 47.5 cm. The used measurement antenna is a R&S®TC-TA85 cross-polarized Vivaldi antenna. The complete setup is designed for direct FF as well as near-field radiation pattern measurements from 18 to 87 GHz.

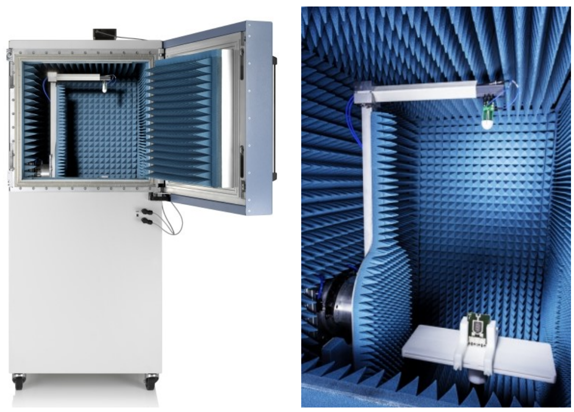

Fig. 4. R&S®ATS1000 fully anechoic chamber from the outside with door open (left) and the inside (right), showing the conical cut system. The DUT represented here is voluntarily not the one which was tested.

The used DUT has a typical mobile handset form factor with ca. 15cm length and 75mm width. It mostly consists of a printed circuit board with printed antennas operating at 28 GHz range. The following section shows test results on one of these antennas. The measurements are conducted by connecting one of the VNA ports to the input of this antenna, with the other DUT ports being connected to 50 Ohm loads. Two other ports of the VNA link to the two measurement probe ports, which respectively allow reception or transmission of orthogonal electric field polarizations.

B. Results

The actual size of the antenna element in the tested DUT is about 7mm. It is located at the top edge of the DUT. In order to elaborate further on the question of the FF testing distance, the DUT FF directivity pattern is tested with the antenna being placed at the center of coordinates of a 6m-range fully anechoic FF chamber (data referred to as "reference" below). The DUT directivity is also assessed with the above-described measurement setup, where the antenna is either positioned at the center of coordinate system, or at a +25mm offset along the DUT main axis (y direction), or at +78mm offset along the y direction. Fig. 5 and Fig. 6 display the measurement results.

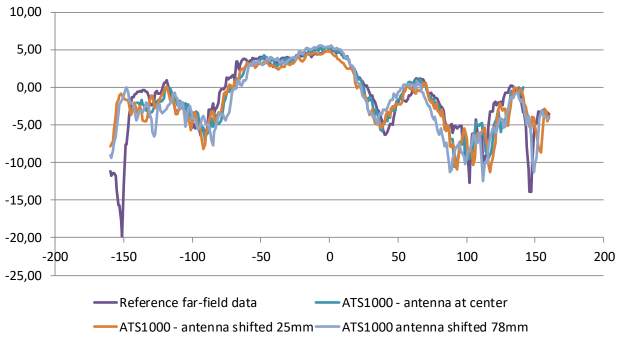

Fig. 5. Directivity data comparisons for the various test conditions in the H-plane (yz).

A good agreement is observed between the patterns in the various test conditions. The effect of a longer testing distance is clearly seen from the depth of the nulls and differences in the structure of the minor lobes of the far-field reference data. Nevertheless, when the antenna is located at the center of the coordinate system, the difference is less than 0.4 dB at the peak beam between the reference and ATS1000 data.

Applying r_{ff} formula by taking D as the complete DUT size would yield a FF distance of about 4m, which, on the presented results, appears clearly over-conservative for evaluating the main beam pattern. By shifting the DUT by 78mm away from the center, the antenna goes out of the supposed ATS1000 quiet zone (traditionally calculated based on phase curvature and r_{ff}). Discussions in previous sections support the idea that this quiet zone definition is too restrictive and that results can still be accurate in the main lobe in the considered test positions. Only an additional error relating to the center of phase being away from the center of coordinates shall be taken into account.

Indeed, in the shifted position, the radiation at ±5° around the peak is overestimated by up to 32% in the H-plane and 25% in the E-plane. A simple correction of the results by the factor $(47.5 - 7.8)/47.5$, which assumes that the measurement probe and DUT are in each other's respective far-field, the errors in the ±5° angles go down to 9% for the H-plane and 5% for the E-plane. This corroborates the fact that the far-field assumption is valid at a measurement distance about seven times shorter that what the classical FF distance formula would define.

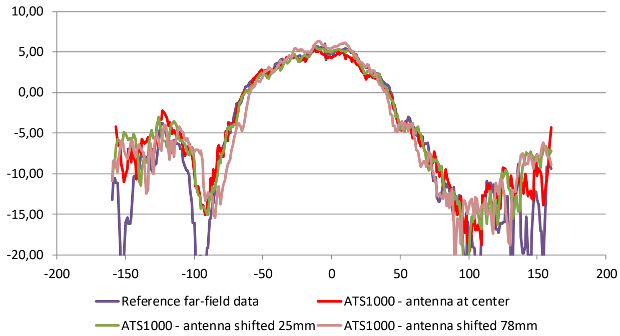

Fig. 6. Directivity data comparisons for the various test conditions in the E-plane (xy).

VI. Conclusion

The theoretical analysis presented in this paper supports the idea that the far-field behavior is formed much earlier in space than classically understood from the well-known $2D^2/\lambda$. Two new expressions for far-field distances based on assumptions on maximum order of excited spherical harmonics are derived which are sufficient for main bean radiation pattern characterization. The additional errors relating to these much shorter distances have been discussed and measurements performed in compact anechoic chamber corroborate the findings. The author intends to provide additional numerical and measurement results in future publications.

Acknowledgment

The author thanks S. Schmitz, Prof. C. Rowell, Dr. A. Tankielun and Dr T. Hertel at Rohde & Schwarz for the excellent interactions and fruitful discussions on antenna testing. The author would like to give a special thank to Prof. Wen Geyi at Nanjing University of Information Science & Technology, for the excellent long-term inspiration that his work has been as well as for the great interactions on the topics discussed in this paper.

References

[1] www.3gpp.org

[2] IEEE Standard Test Procedures for Antennas, IEEE Std 149-1979 (R2008).

[3] K. T. Selvan, R. Janaswamy, "Fraunhofer and Fresnel distances," IEEE Antennas Propagat. Magazine, Aug. 2017.

[4] R.F. Harrington, "Effect of antenna size on gain, bandwidth and efficiency," Journal of Research of Nat. Bur. of Stand. – D, Vol 64D, No. 1, Jan. 1960.

[5] R. L. Fante, "Quality factor of general ideal antennas," IEEE Trans. Antennas Propagat., Vol. AP-17, No. 2, March 1969.

[6] P.-S. Kildal, E. Martini, S. Maci, "Degrees of freedom and maximum directivity of antennas," IEEE Antennas Propagat. Magazine, Aug. 2017.

[7] W. Geyi, "A new derivation of the upper bounds for the ratio of gain to Q," IEEE Trans. Antennas Propagat., Vol. 60, No. 7, July 2012.

[8] M. Abramowitz, I. Stegun, *Handbook of mathematical functions*, Dover, 1964, p. 364.

[9] W. Geyi, "Physical limitations of antennas," IEEE Trans. Antennas Propagat., Vol. 51; No. 8, Aug. 2003.